Downloaded from genome.cshlp.org on November 8, 2026 . Published by Cold Spring Harbor Laboratory Press



Genomic determination of the glucocorticoid response reveals unexpected mechanisms of gene regulation

Timothy E. Reddy, Florencia Pauli, Rebekka O. Sprouse, et al.

Genome Res. published online October 2, 2009
Access the most recent version at doi:10.1101/gr.097022.109

P<P Published online October 2, 2009 in advance of the print journal.

Open Access Freely available online through the *Genome Research* Open Access option.

License Freely available online through the Genome Research Open Access option.

Email Alerting Service Receive free email alerts when new articles cite this article - sign up in the box at the top right corner of the article or **click here.**



To subscribe to *Genome Research* go to:
https://genome.cshlp.org/subscriptions

Copyright © 2009 by Cold Spring Harbor Laboratory Press

Downloaded from genome.cshlp.org on November 8, 2026 . Published by Cold Spring Harbor Laboratory Press

Article

Genomic determination of the glucocorticoid response reveals unexpected mechanisms of gene regulation

Timothy E. Reddy,[1] Florencia Pauli,[1] Rebekka O. Sprouse,[1] Norma F. Neff,[2] Kimberly M. Newberry,[1] Michael J. Garabedian,[3] and Richard M. Myers[1,4]

[1]*HudsonAlpha Institute for Biotechnology, Huntsville, Alabama 35806, USA;* [2]*Department of Bioengineering, Stanford University School of Medicine, Stanford, California 94305, USA;* [3]*Departments of Microbiology and Urology, New York University School of Medicine, New York, New York 10016, USA*

The glucocorticoid steroid hormone cortisol is released by the adrenal glands in response to stress and serves as a messenger in circadian rhythms. Transcriptional responses to this hormonal signal are mediated by the glucocorticoid receptor (GR). We determined GR binding throughout the human genome by using chromatin immunoprecipitation followed by next-generation DNA sequencing, and measured related changes in gene expression with mRNA sequencing in response to the glucocorticoid dexamethasone (DEX). We identified 4392 genomic positions occupied by the GR and 234 genes with significant changes in expression in response to DEX. This genomic census revealed striking differences between gene activation and repression by the GR. While genes activated with DEX treatment have GR bound within a median distance of 11 kb from the transcriptional start site (TSS), the nearest GR binding for genes repressed with DEX treatment is a median of 146 kb from the TSS, suggesting that DEX-mediated repression occurs independently of promoter-proximal GR binding. In addition to the dramatic differences in proximity of GR binding, we found differences in the kinetics of gene expression response for induced and repressed genes, with repression occurring substantially after induction. We also found that the GR can respond to different levels of corticosteroids in a gene-specific manner. For example, low doses of DEX selectively induced *PERI*, a transcription factor involved in regulating circadian rhythms. Overall, the genome-wide determination and analysis of GR:DNA binding and transcriptional response to hormone reveals new insights into the complexities of gene regulatory activities managed by GR.

[Supplemental material is available online at http://www.genome.org. The sequence data from this study have been submitted to the NCBI Short Read Archive (http://www.ncbi.nlm.nih.gov/Traces/sra/sra.cgi) under accession no. SRA008630.]

Cortisol, a steroid hormone of the glucocorticoid (GC) class, is one of the major hormonal signals in the human body. GCs have a wide variety of physiological effects, including the regulation of glucose synthesis in response to circadian rhythms and the suppression of inflammation in response to stress. The anti-inflammatory activity of GCs is the basis for pharmaceuticals such as dexamethasone (DEX), a synthetic GC mimic, that are used to treat inflammatory diseases, including rheumatoid arthritis, Crohn's disease, and psoriasis. However, long-term exposure to GCs leads to severe side effects (Orth 1995; Hopkins and Leinung 2005), and a detailed understanding of the biological mechanisms involved may pave the way for more targeted anti-inflammatory treatments.

The GC receptor (GR) (encoded by the *NR3C1* gene)translates the cortisol signal into genomic outputs by binding the ligand and regulating gene expression. In the absence of hormone, GR primarily resides in the cytoplasm in association with the *HSP90*-based chaperone complex (Pratt et al. 2006). Upon entering a cell, GCs bind to GR and trigger a conformational change that releases the *HSP90* complex. GR then translocates into the nucleus where it binds DNA and regulates gene expression. Activation of gene expression occurs by GR recruiting co-activators and the basal transcriptional machinery to initiate transcription. Repression has been shown to occur by a variety of mechanisms, including competitive interactions with other activating transcription factors (De Bosscher et al. 2000) and inhibition of transcription through changes in phosphorylation of the C-terminal domain of RNA polymerase II (Pol II) (Nissen and Yamamoto 2000). However, which of these mechanisms are most used in vivo remains unknown.

Many researchers have identified DEX-responsive genes in a variety of cell types. Early discoveries include the induction by GR of *NFKBIA* (*IκBα*), an important inhibitor of *NFKB*-mediated inflammation (Auphan et al. 1995; Scheinman et al. 1995; Rhen and Cidlowski 2005), as well as GC-regulated genes involved in apoptosis (Viegas et al. 2008), cell cycle progression (Rogatsky et al. 1997), circadian rhythms (Balsalobre et al. 2000), and intercellular signaling (Chinenov and Rogatsky 2007). Recently, hybridization to microarrays was used to identify 71 DEX-responsive genes, and chromatin immunoprecipitation (ChIP) followed by microarray hybridization (ChIP-array or ChIP-chip) experiments revealed that many of the genes exhibit GR:DNA binding near the transcription start site (TSS) (Wang et al. 2004; So et al. 2007). While numerous DEX-responsive genes and related GR binding sites have been identified, a comprehensive map of GR binding sites and GC-responsive genes throughout the human genome, critical to understanding the genomic GC response, has not yet been produced.

Recent advances in next-generation DNA sequencing, in which millions of short (25–50 nucleotides [nt]) sequence tags can be rapidly generated, have enabled new techniques to measure protein:DNA binding (ChIP with massively parallel sequencing [ChIP-seq]) and gene expression (RNA-seq) with much greater depth,

[4]**Corresponding author.**
E-mail rmyers@hudsonalpha.org; fax (256) 327-0978.
Article published online before print. Article and publication date are at http://www.genome.org/cgi/doi/10.1101/gr.097022.109. Freely available online through the *Genome Research* Open Access option.

Downloaded from genome.cshlp.org on November 8, 2026 . Published by Cold Spring Harbor Laboratory Press

accuracy, and dynamic range than is possible using array-based hybridization approaches. Unlike ChIP-chip and ChIP-PCR assays, sequencing-based ChIP-seq does not require a priori information about the location of potential binding sites and thus can be used to generate comprehensive high-resolution maps of transcription factor binding across the entire genome of any organism with a reference genomic sequence (Robertson et al. 2007; Valouev et al. 2008). Likewise, determining the transcriptome with RNA-seq provides a way to obtain gene expression profiles at a higher level of detail, accuracy, and complexity than is possible with microarray hybridization (Cloonan et al. 2008; Mortazavi et al. 2008). The information obtained by coupling these two approaches, ChIP-seq and RNA-seq, allows well-studied systems to be examined at much greater depth and detail, thus revealing new insights into their overall behavior.

Motivated by the biological and clinical significance of GR-mediated gene regulation, we used ChIP-seq and RNA-seq to produce a comprehensive genomic map of GR:DNA binding and gene regulation in the human A549 lung epithelial carcinoma cell line in response to treatment with DEX. By combining GR binding and gene expression data, we characterized genome-wide GR binding and found unexpected differences between the activating and repressive functions of the GR, as well as a striking dosage difference in a key gene involved in circadian cycles.

Results

Comprehensive identification of GR occupancy with ChIP-seq

We used ChIP-seq to identify the genomic locations bound by GR in human A549 lung epithelial carcinoma in response to DEX treatment. We isolated DNA from immunoprecipitated chromatin samples from A549 cells treated for 1 h with either 100 nM DEX or ethanol, as a control. We sequenced the ChIP DNA with an Illumina Genome Analyzer (Supplemental Table S1) and aligned the sequence reads to the human genome by using the ELAND program (Illumina). We then used the MACS algorithm with a 2% false-discovery rate (FDR) to call peaks in the aligned sequence data (Zhang et al. 2008), and identified 4392 genomic positions that became occupied by GR upon DEX treatment. By comparing an earlier ChIP-chip study that identified 73 GR binding sites (So et al. 2007), we reproduced 65 of the previously identified sites (89%). Finally, by using ChIP-QPCR to validate a selection of 42 GR binding sites that represent the full range of observed signal strength, we observed strong correlation (r^2 = 0.71) in the level of DEX-induction between the two assays (Supplemental Fig. S1).

The GR preferentially bound in regions upstream of TSSs and in first intron of genes (Fig. 1A), which together comprised 22% of the identified binding sites. Absent DEX, we commonly found low levels of GR ChIP-seq signal. Such signal may be the result of GR binding due to hormones in cell growth serum and from the GR cycling through the nucleus in the absence of cortisol (Young and Hartl 2002). Sequencing bias toward open chromatin (Auerbach et al. 2009) may also contribute to signal at these regions (John et al. 2008). Overall, DEX treatment induced a median 11-fold increase in ChIP-seq signal across all binding sites (Supplemental Figs. S2, S3). However, the level of GR signal in the absence of DEX only weakly correlated with the strength of GR signal after the addition of DEX (r^2 = 0.11). A complete list of binding sites at all significance thresholds is available in data set 1.

GR binds DNA either directly at a GC response element (GRE) or indirectly via another factor such as AP-1, and the binding is thought to lead to activation or repression of gene expression

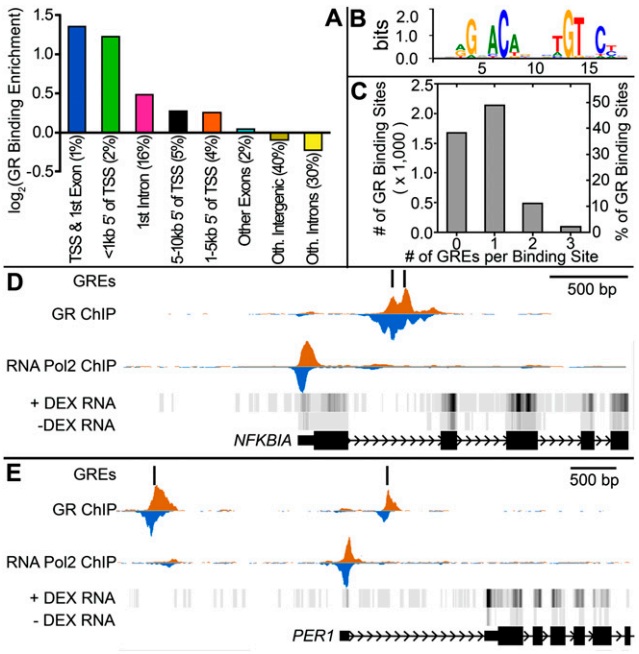


Figure 1. Genomic distribution of glucocorticoid receptor binding sites and response elements. (*A*) Enrichment of GR binding sites in genomic features. The percentage of all identified GR binding sites in each type of region, indicated in parentheses, was divided by the relative amount of the human genome each type of region occupies and plotted on a $\log_2$ scale. (*B*) The revised glucocorticoid response element (GRE) identified in the most significant GR binding sites identified by ChIP-seq. (*C*) Distribution of the number of GREs in identified high-confidence GR binding sites across the human genome. (*D*,*E*) Example ChIP-seq data showing GR and Pol II (RNA Pol2) binding at GREs near the *NFKBIA* and *PER1* genes. ChIP-seq data are plotted as the density of 25-bp tags mapping to the region. The density is separated to show reads mapping to the positive (orange) and negative (blue) strand of the reference genome. For RNA-seq data, darker indicates more expressed.

(Deblois and Giguere 2008). While the GRE sequence is most commonly reported as the 6-bp inverted repeat 5′-AGAACA nnnTGTTCT-3′ (Strähle et al. 1987), others have noted conserved variation in the DNA sequences bound by GR (La Baer and Yamamoto 1994; So et al. 2008; Meijsing et al. 2009). To refine the GRE, we performed in silico binding motif identification on the 100 most significant GR binding sites determined by the MACS peak caller, and we further refined the identified motif across the 500 most significant sites. The GRE we defined with these new data showed the expected structure of a 6-bp inverted repeat separated by three nonspecific bases (Fig. 1B). The identified motif, with the half-site sequence RGnACA, agrees very well with that reported earlier from detailed biochemical studies (La Baer and Yamamoto 1994). By mapping the motif against occupied sites in our genome-wide analysis, we found that 2715 (62%) of the DEX-induced GR binding sites contain at least one GRE (Fig. 1C). A weak but significant correlation exists between the number of binding motifs in a site and the strength of the site (r^2 = 0.051, $P < 2.2 \times 10^{-16}$). Notably, for the *NFKBIA* gene, a major component of the anti-inflammatory response that is up-regulated by GCs, we identified two GR-bound GREs in the first intron of the *NFKBIA* gene, likely explaining the well-known up-regulation of *NFKBIA* in response to GCs (Fig. 1D).

By further testing for overrepresented DNA sequence motifs in ChIP-seq peaks that lack a GRE, we identified the DNA binding

Downloaded from genome.cshlp.org on November 8, 2026 . Published by Cold Spring Harbor Laboratory Press

motif of the AP-1 transcription factor, a well-known transcriptional cofactor of the GR (Herrlich 2001). Overall, 32% of the sites of GR occupancy contain a consensus binding sequence for AP-1. Sites of GR binding that lack a GRE are slightly more likely to contain an AP-1 site (36%) compared with the GR binding sites that contain a GRE (29%), and may explain some of the ChIP-seq signal at the GRE-less sites.

Identification of GC-responsive genes by RNA-seq

We used RNA-seq (Mortazavi et al. 2008) to measure transcript abundance in DEX-induced and uninduced A549 cells. We isolated mRNA from A549 cells treated for 1 h either with 100 nM DEX or with ethanol, reverse transcribed the mRNA into cDNA, and sequenced the cDNA on an Illumina Genome Analyzer (Supplemental Table S2). After aligning data to the reference genome and exon–exon junctions, we used the ERANGE software (Mortazavi et al. 2008) to calculate expression of 29,673 genes in units of reads per kilobase of exon per million sequence tags (RPKM). Overall, we found that 11,926 (40%) genes were expressed above our minimum threshold of 1 RPKM in at least one mRNA determination. We identified 234 genes with a significant (FDR < 5%) change in expression in response to DEX treatment. After removing pseudogenes (listed in Supplemental Table S3), 209 differentially expressed genes remained (Fig. 2A). Of the DEX-responsive genes, more showed increases in transcript levels (59%) than showed decreases (41%), and the up-regulation was slightly but significantly stronger than the down-regulation (P = 0.003, one-sided Mann-Whitney U-test). To confirm the RNA-seq measurements, we measured expression response of 87 of the DEX-responsive genes with RT-QPCR. Of the genes we tested, 84 (97%) showed a change in expression in the same direction as measured by RNA-seq, and we observed strong correlation (r^2 = 0.86) between the RT-QPCR and RNA-seq measurements (see data set 2). As an additional validation, we performed ChIP-seq with antibodies targeted to Pol II. Overall, 94% of the DEX-responsive genes show a change in Pol II ChIP-seq signal in the same direction as the measured gene expression response. The correspondence was slightly higher (98%) when we used an antibody targeted to a serine-2 phosphorylated C-terminal domain of Pol II that is associated with transcriptional elongation. Despite strong correspondence between direction of changes in gene expression and in Pol II ChIP-seq signal, the correlation between the magnitude of relative expression and magnitude of relative ChIP-seq signal is weak for both general Pol II (r^2 = 0.10, $P = 2 \times 10^{-6}$) and for the serine-2 phosphoisoform (r^2 = 0.12, $P = 5.8 \times 10^{-7}$).

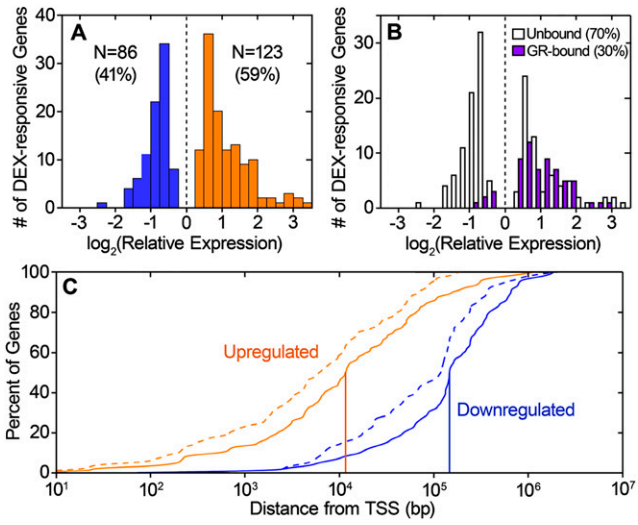


Figure 2. Gene expression response to dexamethasone and overlap with glucocorticoid receptor binding. (*A*) Histogram showing the distribution of expression change for the DEX-responsive genes, as measured with RNA-seq. DEX-induced genes are shown in orange, while DEX-repressed genes are shown in blue. (*B*) Comparison of DEX response in genes that have GR binding within 10 kb of their transcription start site (purple) and genes without GR binding in the same region (white). (*C*) Percentage of DEX-responsive genes (*y*-axis) that have GR binding within a given distance from the transcription start site (*x*-axis). Orange line, up-regulated genes; blue line, down-regulated genes. Vertical lines indicate median distance to nearest binding site. Dashed lines indicate binding sites called with a lower confidence threshold of FDR < 5%.

Finally, combining data from RNA-seq and Pol II ChIP-seq in A549 cells, we identified the predominantly expressed splice isoform for each of the DEX-responsive genes. For two of the DEX-responsive genes (*BBC3* and *FGD4*), the Pol II ChIP-seq data and the RNA-seq data suggest a TSS that does not correspond with a known gene model (Supplemental Figs. S4, S5). In these two cases, we use the position of maximum Pol II ChIP-seq signal as the TSS for all downstream analysis of GR occupancy. A complete list of DEX-responsive genes and corresponding RPKM measurements, along with RT-QPCR validation results for the 87 selected genes and a list of the most prominent splice isoform for each gene, is in data set 2.

Microarray measurements performed on DEX-treated A549 cells previously identified 71 DEX-responsive genes (Wang et al. 2004), 59 (83%) of which were expressed above our minimum expression threshold. We confirmed 37 of the previously identified genes at our significance threshold (FDR < 5%) and identified an additional 19 that did not meet our significance criteria, giving an overall 95% validation rate. Including genes with measured expression of less than 1 RPKM, we found similar changes for 65 (92%) of the previously identified genes. Finally, we identified an additional 172 DEX-responsive genes not reported by Wang et al. (2004).

The DEX-responsive genes that we identified are primarily implicated in two broad classes: stress response and development (Table 1; Reimand et al. 2007). Comparison to Gene Ontology (GO) categories (Ashburner et al. 2000) revealed that the identified genes are involved in stress response ($P = 6 \times 10^{-11}$), organ development ($P = 5 \times 10^{-15}$), cell differentiation ($P = 1 \times 10^{-11}$), hormone secretion ($P = 4 \times 10^{-7}$), and apoptosis ($P = 5 \times 10^{-12}$). Notably, in many of the categories, there was a strong bias toward up- or down-regulation. For example, 14 of the 17 genes involved in apoptosis were up-regulated, and all four genes involved in the inhibition of hormone secretion were down-regulated. On the other hand, the 49 stress-response genes showed a nearly equal distribution, with 53% of the genes more highly expressed in response to DEX. Thirty-eight of the differentially expressed genes are transcription factors ($P = 7 \times 10^{-12}$), including components of AP-1 (*JUN*, *FOSL1*, and *FOSL2*). Notably, we found that five of the krüppel-like factors (*KLF4*, *KLF5*, *KLF6*, *KLF9*, and *KLF10*) are differentially expressed in response to DEX in A549 cells, suggesting an expanded role of cortisol in early development. Finally, four of the identified genes (*PER1*, *PER2*, *CRY2*, and *BHLHE40*) are factors that regulate circadian rhythms ($P = 3.8 \times 10^{-5}$), and help to explain the role of GCs therein. A complete list and details of functional enrichment in DEX-responsive genes is available in data set 3.

Downloaded from genome.cshlp.org on November 8, 2026 . Published by Cold Spring Harbor Laboratory Press

Table 1. GO functional enrichment of DEX-responsive genes

Category (no. of genes)
Anatomical structure development (60)
Anatomical structure morphogenesis (32)
Response to chemical stimulus (27)
Response to external stimulus (29)
Response to stress (49)
Response to wounding (20)
Regulation of gene expression (71)
Regulation of cell size (9)
Regulation of apoptosis (29)
Regulation of signal transduction (23)
Positive regulation of cell proliferation (18)
Regulation of muscle cell differentiation (4)
Negative regulation of cell differentiation (12)
Regulation of phosphorylation (10)
Regulation of transcription from Pol II promoter (31)
Intracellular signaling cascade (36)
Epithelial cell differentiation (6)
Cell fate commitment (9)
Tissue development (16)
Gland development (7)
Organ morphogenesis (21)
Negative regulation of transport (8)
Negative regulation of secretion (6)
Negative regulation of hormone secretion (5)
Enzyme linked receptor protein signaling pathway (16)
Cytokine-mediated signaling pathway (7)
Transcription factor activity (38)
Cytokine-cytokine receptor interaction (13)
TGF-beta Signaling pathway (7)
Circadian rhythm (4)
RHO GTPase:GTP activates downstream effector (5)

Bold entries indicate genes with $P < 1 \times 10^{-10}$.

GR binding of DEX-responsive genes

To investigate the role of GR binding in DEX-mediated gene expression, we searched for GR binding sites within 10 kb of the TSS of DEX-responsive genes. The majority (70%) of DEX-responsive genes show no GR binding within 10 kb of the TSS, indicating the GR often acts in an exclusively distal manner. However, up-regulated genes were much more likely to have proximal GR binding. We observed GR binding near 47% of the induced genes, but near only 8% of the repressed genes (Table 2; Fig. 2B). The lack of GR binding at DEX-repressed genes agrees with previous targeted studies of conserved GR response elements in mouse cells (So et al. 2008). Overall, the GR binds dramatically closer to up-regulated genes than to down-regulated genes, with the nearest sites occurring within a median distance of 11 kb and 146 kb, respectively, of the TSS (Fig. 2C; $P < 2 \times 10^{-16}$, one-sided Mann-Whitney *U*-test). This finding is not due to our 2% FDR threshold, as by repeating the analysis with lower-confidence binding sites (FDR < 5%), we found that the nearest GR binding occurs a median of 6 kb from the TSS of up-regulated genes but 119 kb from the TSS of down-regulated genes (Fig. 2C, dashed lines). We observed no significant correlation between the proximity or the change in GR binding upon addition of DEX and the magnitude of induction of the nearby gene. However, the 20 genes with more than one GR-bound GRE were induced more strongly than genes with a single bound GRE ($P = 8 \times 10^{-3}$, one-sided U-test), indicating that multiple GR binding sites can produce additive effects. Of the genes with multiple bound GREs, nine contain binding sites both upstream and downstream of the TSS, and they were among the most highly DEX-responsive genes (Table 2, underlined entries). Of the seven repressed genes with a nearby high-confidence binding site, all contain a GRE sequence, suggesting direct DNA:GR binding is involved in the inhibition of a subset of the repressed genes.

Table 2. DEX-responsive genes with nearby GR binding sites

Gene	Log_2(Rel. Exp.)[a]	No. of Peaks	No. of GRE
PER1	**2.54**	**2**	**2**
ZFP36	**2.29**	**2**	**0**
TFCP2L1	1.99	1	1
IGFBP1	1.95	1	3
ANGPTL4	1.92	2	1
BIRC3	**1.87**	**2**	**1**
ENTPD2	1.76	3	2
CIDEC	**1.70**	**2**	**2**
TIPARP	1.69	1	1
BCL6	1.68	1	2
SLC19A2	1.54	1	1
NFKBIA	1.53	1	2
CEBPD	1.49	1	2
SDPR	1.45	1	0
PAMCI	1.44	1	0
C9orf150	1.35	1	0
KLF9	1.35	1	1
RRAD	1.34	1	1
DUSP1	**1.33**	**4**	**3**
ZC3H12A	**1.18**	**2**	**1**
TNFAIP3	1.18	1	0
PARD6B	1.13	2	2
PER2	**1.12**	**3**	**1**
ERN1	1.11	1	0
STOM	1.07	1	1
THBD	1.03	1	2
ALOX5AP	1.02	1	0
ELL2	1.02	1	2
CEBPB	0.98	1	0
EDN2	0.95	2	2
ZNF57	0.85	1	0
PXN	0.83	1	1
FOSL2	0.80	1	1
MT2A	**0.76**	**3**	**4**
ITPKC	**0.74**	**2**	**1**
MT1X	0.74	1	0
CKB	0.71	1	1
TIGD2	0.70	1	0
KIAA1754	0.66	1	1
SLC22A5	0.66	3	1
FAM105A	0.66	1	2
ZFAND5	0.65	1	3
NOL3	0.60	1	1
ARRDC2	0.55	2	0
RHOBTB2	0.54	2	1
ZNF281	0.52	1	1
PPP1R15B	0.47	1	1
LRRC8A	0.47	2	0
RHOB	0.46	1	1
KLF5	0.44	1	1
BAG3	0.44	2	2
SRGN	0.43	1	2
IL6ST	0.42	1	1
AHNAK	0.41	1	1
THBS1	0.40	1	0
EDN1	−0.45	1	1
ID3	−0.46	1	1
FZD2	−0.47	1	1
BDKRB2	−0.52	1	1
MIDN	−0.69	1	1
GDF15	−0.82	1	0

Boldface indicates that GR binds locally on both sides of the TSS.
[a]Log_2(Rel. Exp.) indicates the log_2 of the relative expression of the gene ± DEX treatment.

Downloaded from genome.cshlp.org on November 8, 2026 . Published by Cold Spring Harbor Laboratory Press

Time and dose response of DEX-responsive genes

We next sought to characterize the differences between up-regulation and down-regulation in response to DEX. In addition, we wanted to determine whether certain genes respond to different concentrations of corticosteroids, potentially explaining the role of cortisol in seemingly unrelated physiological processes. To investigate this possibility, we used RT-QPCR to measure expression response of 44 strongly induced or repressed genes at DEX concentrations ranging from 100 pM–1 μM and over treatment times ranging from 5 min to 4 h.

Varying the concentration of DEX, we found that 50% gene expression response (EC_{50}) occurred with 3 nM DEX for both the up- and down-regulated genes (Fig. 3A). Interestingly, *PER1*, a key transcription factor that regulates circadian rhythms, reproducibly responded to sixfold lower concentration of DEX (EC_{50} = 500 pM), and follow-up measurements of different exons and exon–exon junctions confirmed the low-dose response (Fig. 3B,C). Examining the *PER1* promoter in detail, we found two bound GREs flanking the Pol II-occupied TSS. One site is located 500 bp downstream of the TSS, in the first intron, and the other site is in intergenic DNA 2 kb upstream of the TSS (Fig. 1E). While it may be possible that Pol II is poised at the *PER1* promoter prior to DEX treatment, we did not find particularly high Pol II occupancy compared with other similarly induced genes.

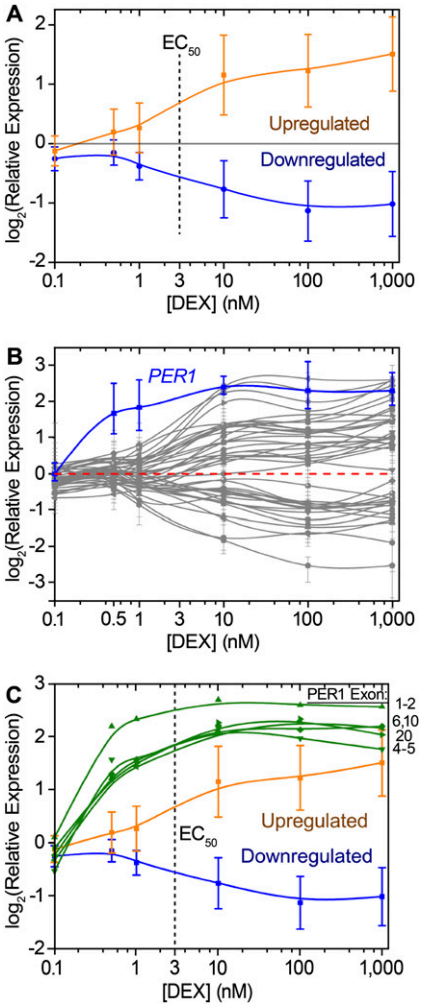


Figure 3. Dose response to dexamethasone. (*A*) Gene expression response, measured with RT-QPCR, of DEX-responsive genes in response to treatment with increasing concentrations of DEX. The up-regulated genes (orange line) and down-regulated genes (blue line) showed similar response, with $EC_{50} \sim$ nM (dashed line). Error bars, SD. (*B*) *PER1* (blue line) is particularly responsive to low concentrations of DEX, compared with all other genes measured (gray lines). Error bars, maximum and minimum over three biological replicates. (*C*) *PER1* dose response (green lines) verified with primers designed against various exons and exon–exon junctions, as indicated. For comparison, the overall response of activated (orange line) and repressed genes (blue line) is reproduced. Error bars, SD.

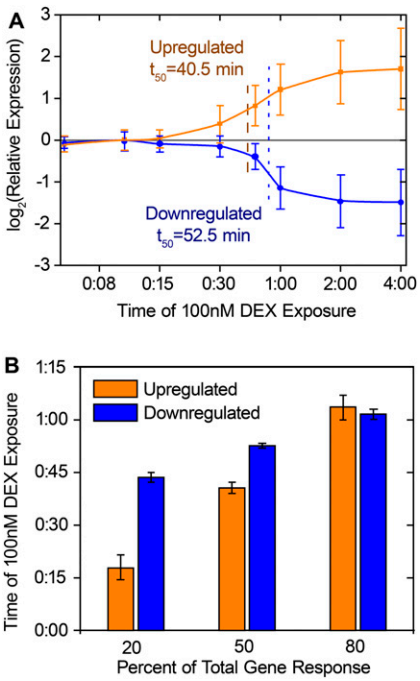


Figure 4. Time-course response to dexamethasone. Gene expression response, measured with RT-QPCR, of DEX-responsive genes over increasing duration of exposure to 100 nM DEX treatment. (*A*) Average gene expression response (*y*-axis) across the time-course (*x*-axis). Error bars, SD. Fifty percent response time for up- and down-regulated genes are indicated with dashed and dotted lines, respectively. (*B*) Time of exposure to 100 nM DEX required to achieve 20%, 50%, and 80% response for up-regulated (orange bars) and down-regulated (blue bars) genes. Error bars, SE in each parameter from curve fitting.

To evaluate the time required for gene-expression response to DEX, we varied the treatment time from 5 min to 4 h, and found substantial differences between up- and down-regulated genes across a set of 44 DEX-responsive genes. For activated genes, 20% and 50% of total response occurred at 18 and 40 min, respectively. In comparison, repression began later but occurred more abruptly, and 20% and 50% repression occurred after 44 and 53 min of DEX exposure (Fig. 4). Overall, the observed kinetics agree well with rapid induction and repression described recently (John et al. 2009). Additionally, the longer time to observe repression may explain the observation that down-regulation after 1 h of DEX treatment was slightly but significantly weaker than up-regulation. Notably, despite responding to low doses of DEX, *PER1* gene expression was not induced earlier than other genes.

Finally, we used inhibition of GR by RNAi to confirm the role of the receptor in the observed expression responses across the same 44 DEX-responsive genes assayed above. We transiently transfected A549 cells with siRNAs specifically targeted to the GR

Downloaded from genome.cshlp.org on November 8, 2026 . Published by Cold Spring Harbor Laboratory Press

or with control siRNAs that do not specifically target any human gene. On average, we observed a twofold decrease of the GR transcript, as measured with RT-QPCR, and stronger reduction of GR protein (Fig. 5A). We then exposed GR and control knockdown cells to DEX and compared the gene expression response. As expected, we found GR knockdown cells had a substantial and significant reduction in DEX response across nearly all genes tested (Fig. 5B). The knockdown abrogated both induction and repression in response to DEX and did not affect genes with proximal GR binding sites differently than genes with exclusively distal sites. Interestingly, the *PER1* response was only sensitive to GR knockdown at low doses, indicating that the full response is robust to even low-levels of GR in the cell (Supplemental Fig. S7).

Discussion

The GR has been extensively studied for more than 50 yr. Here, we present the most comprehensive study to date of GR binding and gene expression throughout the human genome. By using next-generation sequencing to survey DNA fragments isolated from ChIP experiments and mRNA populations, we comprehensively described the DEX response across the entire human genome at nearly single nucleotide resolution. As a result, we identified thousands of heretofore-unknown sites of GR occupancy in A549 cells, a cell line used by many researchers to study the biology of the GC response. Importantly, because ChIP-seq is able to assay the entire genome, we uncovered many new intronic GR binding sites missed by promoter studies, and this may explain the transcriptional response of genes such as *NFKBIA* to DEX. By sequencing the A549 transcriptome with and without DEX treatment, we identified many new and potentially important genes that are responsive to GCs.

While GR binding to DNA can activate and repress gene expression (De Bosscher and Haegeman 2009), combining our GR binding data with measurements of gene expression response showed that the majority of down-regulation occurs independently of proximal GR–DNA interactions. Furthermore, kinetic evaluation shows that repression occurs more slowly than activation. One explanation is that GR-mediated repression involves long-range *cis*-interactions. However, one might also expect such interactions would become fixed with cross-linking, and would appear as binding sites in ChIP-seq. Instead, our results give emphasis to the role of protein–protein interactions that occur away from the DNA (McEwan et al. 1997). Meanwhile, others have noted that new protein synthesis is necessary for DEX-mediated repression in some instances (Auphan et al. 1995). With the large cohort of transcriptional regulators differentially expressed with DEX treatment, and fitting nicely with the observed time delay between activation and repression, we may find that secondary effects are the most prominent mechanism of gene repression in response to GCs. Similarly, our RNA-seq approach will not detect expression of microRNAs, and these molecules may also contribute to secondary repressive effects.

Another striking finding in our study is the low-dose GC response of *PER1*. While *PER1* has been shown to be a GR target gene in mouse (Yamamoto et al. 2005), the response to low-level hormone has not been described. The mechanism by which the GR can activate specific genes at low doses of GC is not yet understood. In principle, the number, affinity, and/or location of the *PER1* GREs might preferentially lead to response at low hormone concentrations when only a fraction of the GR is activated. However, other genes such as the related *PER2* transcription factor have a similar number and arrangement of GREs and respond similarly to 100 nM DEX treatment, but do not exhibit the low dose response, suggesting other mechanisms. Recent work from the Yamamoto laboratory (Meijsing et al. 2009) demonstrated that subtle changes in the GRE sequence impart unique structural characteristics to GR that affect its activity. This dispels the simple notion that GRE binding affinity and response are directly coupled. Instead, it appears that the DNA sequence itself acts as a ligand to affect GR function, and this mechanism could explain the low-dose response of the *PER1* locus. Alternatively, the GR is well known to interact with other nuclear receptors such as the mineralocorticoid receptor (MR) (Pearce and Yamamoto 1993), and it is also possible that the MR or another nuclear receptor is contributing to the sensitivity of *PER1* to DEX. Regardless of the mechanism, it is likely that additional GR target genes sensitive to low dose GCs exist but have escaped detection because of the higher levels of hormones prominently used here and elsewhere.

Finally, the detailed characterization of the DEX response presented here may help further our understanding of disease and development. For example, among the DEX-responsive genes are groups of genes that contribute to susceptibility for leukemia (*MCL1* and *FOXN2*, activated; *LIF*, repressed), lymphoma (*BCL6* and *TSPYL2*, activated; *BCL3*, repressed), and psoriasis (*PSORS1C1* and *PSORS1C2*, both activated). We also found that 36 DEX-induced or DEX-repressed genes are involved in intracellular signaling ($P = 2 \times 10^{-8}$). In particular, products of 17 DEX-responsive genes are secreted proteins, many of which have not been previously reported to respond to GCs. These include

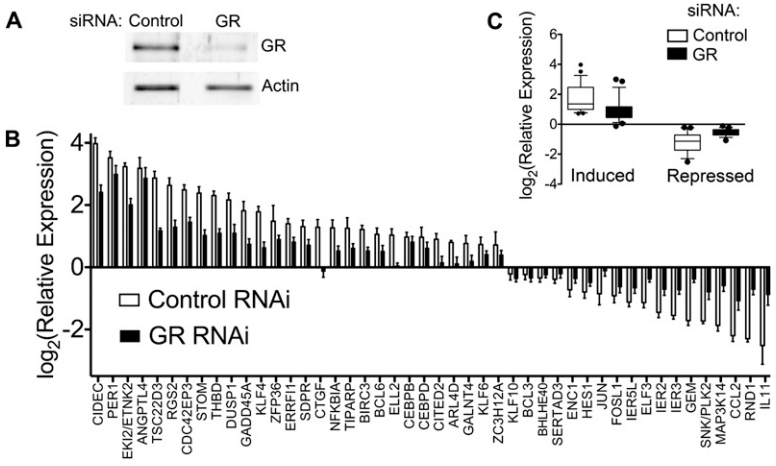


Figure 5. Effect of glucocorticoid receptor knockdown on dexamethasone response. (*A*) Western blot showing the effect of siRNA-mediated knockdown on GR protein levels. (*B*) Gene expression response of 46 DEX-responsive genes to 5-h 100 nM DEX treatment in cells transfected either with control (white bars) or GR-targeting (black bars) siRNA pools. Three independent knockdown experiments were performed for each of two siRNA pools. Error bars, SEM across all six measurements. Measurements for each siRNA pool are available in Supplemental Figures S6 and S7. (*C*) Box plot showing overall effect of siRNA-mediated knockdown of the GR on the gene expression response for DEX-induced and DEX-repressed genes. Whiskers indicate 10%-90% range.

Downloaded from genome.cshlp.org on November 8, 2026 . Published by Cold Spring Harbor Laboratory Press

the leukemia inhibitory factor (*LIF*), a protein commonly used to drive human embryonic stem cells toward differentiation (Smith et al. 1988; Niwa et al. 1998), and follistatin (*FST*), a gene known to function in development and morphogenesis (Matzuk et al. 1995). Both *LIF* and *FST* are repressed with DEX treatment. Combined with our observed DEX response of many developmental transcription factors, including the activation of *POU5F1*(*OCT4*) and *KLF4* and the repression of *SOX2* (Takahashi and Yamanaka 2006), the findings suggest new hypotheses for a role of cortisol in early development.

In summary, our results highlight the ability of high-throughput sequencing–based assays to give broad new genomic and biological insights into previously well-studied systems. As a result, numerous new questions present themselves. For example, this and other studies have shown that the vast majority of transcription factor binding occurs distant from a recognizable genomic feature and possibly has no direct effect on transcription. It remains to be shown if the distal binding events are functional, perhaps through DNA looping, or are simply random events with no evolutionary consequence. Alternatively, many of the binding events may not be important to regulate a specific gene but may instead be used to titrate the amount of the transcription factor that is available in the nucleus, thus creating a system that is more tunable and robust to random environmental perturbations.

Finally, cortisol is known to have broad and diverse effects throughout the body, and there is likely much to be learned by evaluating differences in GR occupancy and related gene expression in other cortisol-responsive tissues and primary cells. Here, the targeted activation of genes at low doses of cortisol may have important physiological implications by directing cortisol response to specific subsets of genes in different tissues based on the endogenous GR levels and the amount of cortisol able to reach that tissue.

Methods

Cell growth and harvest

We grew A549 cells (ATCC CCL-185) in F-12K media (Invitrogen) supplemented with 10% fetal bovine serum (Hyclone) and 1% penicillin-streptomycin (Invitrogen). We passaged and harvested cells at approximately 80% confluence. Prior to harvest, we treated cells for 1 h with either 100 nM DEX in ethanol or an equal volume (0.02% v/v of media) of ethanol as a vehicle control.

For ChIP experiments, we covalently cross-linked protein–DNA complexes by incubating cells in 1% formaldehyde for 10 min at room temperature, followed by incubation in 0.125 M glycine for 5 min to quench the cross-linking reaction. After washing the cells with PBS (pH 7.4) (Invitrogen), they were lysed and scraped in Farnham lysis buffer (5 mM PIPES at pH 8.0, 85 mM KCl, 0.5% NP-40) with added protease inhibitor (Roche). We centrifuged the cell lysate at 1200 rpm for 5 min at 4°C, and stored the crude nuclear extract contained in the supernatant at −80°C.

To prepare RNA samples, we lysed cells with Qiagen buffer RLT with 1% β-mercaptoethanol. We homogenized the lysate by pulling it through a 20-gauge needle 20 times and then snap froze it in liquid nitrogen. We extracted total RNA with Qiagen RNeasy Midi spin columns, including an on-column DNA digestion step.

Chromatin immunoprecipitation

We resuspended four aliquots of 2×10^7 nuclei in 1 mL of RIPA buffer (1% NP-40, 0.5% sodium deoxycholate, 0.1% SDS in PBS at pH 7.4) and fragmented chromatin to 200–500 bp with six pulses of 30 sec at 60% power with a Sonics VibraCell sonicator at 4°C. To remove insoluble components, we centrifuged the samples at 15,000 rpm for 15 min and recovered the supernatant.

We conjugated rabbit polyclonal antibodies specific to the N terminus of mouse GR alpha isoform protein (Santa Cruz Biotechnology sc-1004) or the POLR2A subunit of Pol II (Covance 8WG16 and Abcam ab5095) to goat anti-rabbit or goat anti-mouse IgG magnetic beads (Invitrogen) according to the manufacturer's recommendation. For each aliquot of 2×10^7 nuclei, we added 5 μg of primary antibody to 50 μL of magnetic bead slurry and then added the sheared chromatin in RIPA and incubated on a rotator overnight at 4°C. After incubation, we washed the beads five times with a LiCl wash buffer (100 mM Tris at pH 7.5, 500 mM LiCl, 1% NP-40, 1% sodium deoxycholate) and removed remaining ions with a single wash with 1 mL of TE (10 mM Tris-HCl at pH 7.5, 0.1 mM Na_2EDTA) at 4°C. We eluted chromatin and antibodies from beads by incubating for 1 h at 65°C in IP elution buffer (1% SDS, 0.1 M $NaHCO_3$), followed by incubating overnight at 65°C to reverse formaldehyde cross-links. We extracted proteins with a 25:24:1 solution of phenol:chloroform:isoamyl alcohol (Invitrogen), and further purified the DNA with a spin column (Qiagen), eluting in EB (10 mM Tris-Cl at pH 8.5).

ChIP-seq

For each experiment, we prepared 200–500 ng ChIP DNA for sequencing on the Illumina Genome Analyzer as described (Valouev et al. 2008). In brief, we blunted and ligated ChIP DNA fragments to sequencing adapters and amplified the products with 15 rounds of PCR. We electrophoresed the amplified products on a 1.5% NuSieve GTG low-melt agarose gel (Lonza) for 1.5 h. We excised DNA fragments 150–300 bp in length from the gel and purified them with a Qiagen Gel Extraction kit. We treated the DNA with an additional 25 rounds of PCR. We sequenced the resulting DNA library on the Illumina Genome Analyzer. We filtered reads with the default Illumina chastity filter during the base-calling process, which helps to ensure the quality of the generated sequence. We used ELAND (Illumina) to align 25-bp reads to the human genome (hg18), allowing up to two mismatches per read.

We performed all experiments in biological duplicate, starting from independent cell growth. After verifying that duplicate experiments showed extremely high similarity (>95% concordance across genomic TSSs), we combined results from biological replicates into a single data set. We generated at least 12 million aligned reads for each replicate, giving a total of more than 24 million aligned reads for each ChIP-seq experiment.

We resolved reads that mapped to two to 10 places in the human genome to a unique location according to a Boltzmann distribution weighted by the number of unique reads in a 300-bp window around each region. We used the Boltzmann distribution because it allows compromise between assigning all reads to the most likely location and assigning reads equally to all possible positions. Here, we chose a temperature parameter ($t = 0.005$) that gave strong bias toward assigning all reads to the region with the most unique reads, but produced degeneracy when regions had similar numbers of reads.

Peak calling for ChIP experiments

Regions of TF binding were identified with the MACS peak caller (Zhang et al. 2008). MACS calls binding sites by comparing the density of reads at a genomic location in the ChIP-seq experiment to a local Poisson background density model fit to background reads. Here, the background model was fit to reads from GR ChIP-seq in ethanol-treated cells. To assess statistical significance, MACS

Downloaded from genome.cshlp.org on November 8, 2026 . Published by Cold Spring Harbor Laboratory Press

estimates a FDR by swapping the signal and background datasets, and repeating the peak calling process. We chose for analysis peaks with FDR < 2%.

To evaluate GR binding absent DEX, we sequenced DNA isolated from cross-linked and sonicated chromatin that was not immunoprecipitated, and called peaks in the GR ChIP from ethanol-treated cells relative to total chromatin sequencing. Using the same 2% FDR as above, we only identified 15 binding sites. However, at a more lenient 3% FDR, we identify 2623 binding sites that almost entirely overlap the set of induced GR binding sites. Because the GR binding sites have much less signal in the absence of DEX, it is not surprising that a more lenient significance criterion was needed.

Binding motif identification

To revise the GRE, we first collected the reference-genome sequences for the 100 most significant GR binding sites. We used the dust filter to mask regions of low complexity (RL Tatusov and DJ Lipman, unpubl.) and then used BioProspector (Liu et al. 2001) to search for a 15-bp motif. Following initial motif detection, we used BioOptimizer (Jensen and Liu 2004) to refine each motif further over the 500 most significantly bound sites. Finally, to identify instances of binding motifs in binding sites, we used MAST (Bailey and Gribskov 1998) without an E-value threshold.

RNA-seq

We performed RNA-seq according to the method described by Mortazavi et al. (2008). Briefly, we double-selected polyA-containing mRNA from total RNA by using oligo-dT magnetic beads. To mitigate 3′ bias in mRNA sequencing, we fragmented the mRNA with RNA fragmentation buffer (200 mM Tris-acetate at pH 8.1, 500 mM potassium-acetate, 150 mM magnesium-acetate) and removed free-ions with a G-50 Sepharose spin column. Fragmented mRNA was used as a template to synthesize single-stranded cDNA with SuperScript II reverse transcriptase with random hexamer primers in the presence of RNAseOUT (Invitrogen). We synthesized double-stranded DNA in a modified buffer of 500 mM Tris-HCl (pH 7.8), 50 mM $MgCl_2$, and 10 mM DTT (Illumina).

To prepare dsDNA for sequencing, we ligated sequencing adapters to blunted dsDNA and electrophoresed the products on a 1.5% NuSieve GTG agarose gel (Lonza). We excised fragments between 200 and 250 bp in length from the gel and purified the fragments with the Qiagen Gel Extraction kit according to the manufacturer's protocol. As a final step, we amplified the dsDNA library with 15 rounds of PCR with Illumina sequencing primers.

We mapped reads to the hg18 reference genome by using ELAND (Illumina), allowing up to two mismatches per read, and reported reads that map to 10 or fewer locations. By using the ERANGE software package, we placed uniquely mapped reads against 29,673 transcripts from NCBI build 36.1 of the human genome. After placing unique reads, ERANGE assigned multiply mapping reads and reads mapping to splice junctions according to the number of unique reads in potential transcripts. Once all reads were mapped, ERANGE reported gene expression in units of reads per kilobase of exon and per million tags sequenced (RPKM).

As expected, measurements of gene expression for lowly expressed genes were more variable between biological replicates. To remove the dependence of variance on expression level, we used variance stabilization (Durbin et al. 2002) to transform RPKM values. After the transformation, we calculated ΔH values (the variance stabilization analog of log-ratios) between replicate experiments and between conditions. The ΔH values for biological replicate experiments approximately follows a normal distribution (Supplemental Fig. 1). We fit a normal distribution to the background variance by using maximum likelihood and calculated the probability that an observed change in gene expression occurred by random change, a *P*-value. Finally, we used QVALUE (Storey and Tibshirani 2003) to convert *P*-values to a FDR, and report genes with FDR less than 5%.

To confirm RNA-seq results, we selected a set of 87 genes for RT-QPCR. Genes were selected to cover activated and repressed genes, with a particular focus on genes that showed GR biding near the TSS in our ChIP-seq experiments.

Reverse-transcription quantitative PCR (RT-QPCR)

We extracted total RNA from A549 cells treated for 1 h with DEX (100 pM, 500 pM, 1 nM, 10 nM, 100 nM, or 1 μM) or with 0.02% volume of ethanol as a vehicle control, as described above. We synthesized first-strand cDNA from DNase I–treated RNA with SuperScript II reverse transcriptase with random hexamer primers in the presence of RNAseOUT (Invitrogen), followed by an RNAseH treatement. We purified cDNA with PCR cleanup spin columns (Qiagen). We performed quantitative-PCR with a DyNAmo SYBR green qPCR master mix (Finnzymes F-415 or F-410) and measured quantitative fluorescence on a BioRad iCycler. We normalized genes to beta-actin (ACTB) mRNA and calculated relative expression at each DEX dosage compared with vehicle control cells by using the $\Delta\Delta C_T$ method. We performed all measurements in biological triplicates and reported the average values, along with the minimum and maximum. We calculated EC_{50} values according to a Hill curve fit to dose-response measurements.

RNAi knockdown of GR

We seeded A549 cells in 24-well plates and grew them in antibiotic-free medium overnight to 50% confluence. We washed cells and incubated them for 12 h in serum-free and antibiotic-free medium with 1.5 μL of Santa Cruz Biotechnology transfection reagent (sc-29528) and 1 μL of 10 μM siRNA pool either targeted to the GR (either Santa Cruz Biotechnology sc-35505 or Dharmacon SMARTpool) or designed not to target the human genome (Santa Cruz Biotechnology sc-37007). After incubation, cells were allowed to grow for an additional 48 h in complete media, after which we harvested RNA with RNeasy Micro spin columns (Qiagen) or lysed cells in RIPA buffer for Western blotting.

Acknowledgments

We thank Gavin Sherlock, Barbara Wold, Alayne Brown, Jason Gertz, and Natalie Simpson for their helpful suggestions and critical reading of the manuscript; Chris Partridge and Amy Woodall for their help with experiments; Ali Mortazavi and Brian Williams for their help with RNA-seq; and Jason Dilocker, Mike Muratet, Barbara Pusey, and Rami Rauch and for their work on the sequencing data generation. This work was supported by a grant from the NHGRI as part of the ENCODE Project (NIH 1U54HG004576) and by funds from the HudsonAlpha Institute and by Philip Morris USA Inc. and Philip Morris International (M.J.G.).

References

Ashburner M, Ball CA, Blake JA, Botstein D, Butler H, Cherry JM, Davis AP, Dolinski K, Dwight SS, Eppig JT, et al. 2000. Gene ontology: Tool for the unification of biology. The Gene Ontology Consortium. *Nat Genet* **25:** 25–29.

Downloaded from genome.cshlp.org on November 8, 2026 . Published by Cold Spring Harbor Laboratory Press

Auerbach RK, Euskirchen G, Rozowsky J, Lamarre-Vincent N, Moqtaderi Z, Lefrancois P, Struhl K, Gerstein M, Snyder M. 2009. Mapping accessible chromatin regions using Sono-Seq. *Proc Natl Acad Sci* **106:** 14926–14931.

Auphan N, DiDonato JA, Rosette C, Helmberg A, Karin M. 1995. Immunosuppression by glucocorticoids: Inhibition of NF-kappaB activity through induction of I kappaB synthesis. *Science* **270:** 286–290.

Bailey TL, Gribskov M. 1998. Combining evidence using *P*-values: Application to sequence homology searches. *Bioinformatics* **14:** 48–54.

Balsalobre A, Brown SA, Marcacci L, Tronche F, Kellendonk C, Reichardt HM, Schutz G, Schibler U. 2000. Resetting of circadian time in peripheral tissues by glucocorticoid signaling. *Science* **289:** 2344–2347.

Chinenov Y, Rogatsky I. 2007. Glucocorticoids and the innate immune system: crosstalk with the toll-like receptor signaling network. *Mol Cell Endocrinol* **275:** 30–42.

Cloonan N, Forrest AR, Kolle G, Gardiner BB, Faulkner GJ, Brown MK, Taylor DF, Steptoe AL, Wani S, Bethel G, et al. 2008. Stem cell transcriptome profiling via massive-scale mRNA sequencing. *Nat Methods* **5:** 613–619.

Deblois G, Giguere V. 2008. Nuclear receptor location analyses in mammalian genomes: From gene regulation to regulatory networks. *Mol Endocrinol* **22:** 1999–2011.

De Bosscher K, Haegeman G. 2009. Minireview: Latest perspectives on antiinflammatory actions of glucocorticoids. *Mol Endocrinol* **23:** 281–291.

De Bosscher K, Vanden Berghe W, Haegeman G. 2000. Mechanisms of anti-inflammatory action and of immunosuppression by glucocorticoids: Negative interference of activated glucocorticoid receptor with transcription factors. *J Neuroimmunol* **109:** 16–22.

Durbin BP, Hardin JS, Hawkins DM, Rocke DM. 2002. A variance-stabilizing transformation for gene-expression microarray data. *Bioinformatics* **18** (Suppl 1)**:** S105–S110.

Herrlich P. 2001. Cross-talk between glucocorticoid receptor and AP-1. *Oncogene* **20:** 2465–2475.

Hopkins RL, Leinung MC. 2005. Exogenous Cushing's syndrome and glucocorticoid withdrawal. *Endocrinol Metab Clin North Am* **34:** 371–384 ix.

Jensen ST, Liu JS. 2004. BioOptimizer: A Bayesian scoring function approach to motif discovery. *Bioinformatics* **20:** 1557–1564.

John S, Sabo PJ, Johnson TA, Sung MH, Biddie SC, Lightman SL, Voss TC, Davis SR, Meltzer PS, Stamatoyannopoulos JA, et al. 2008. Interaction of the glucocorticoid receptor with the chromatin landscape. *Mol Cell* **29:** 611–624.

John S, Johnson TA, Sung MH, Biddie SC, Trump S, Koch-Paiz CA, Davis SR, Walker R, Meltzer PS, Hager GL. 2009. Kinetic complexity of the global response to glucocorticoid receptor action. *Endocrinology* **150:** 1766–1774.

La Baer J, Yamamoto KR. 1994. Analysis of the DNA-binding affinity, sequence specificity and context dependence of the glucocorticoid receptor zinc finger region. *J Mol Biol* **239:** 664–688.

Liu X, Brutlag DL, Liu JS. 2001. BioProspector: Discovering conserved DNA motifs in upstream regulatory regions of co-expressed genes. *Pac Symp Biocomput* **2001:** 127–138.

Matzuk MM, Lu N, Vogel H, Sellheyer K, Roop DR, Bradley A. 1995. Multiple defects and perinatal death in mice deficient in follistatin. *Nature* **374:** 360–363.

McEwan IJ, Wright AP, Gustafsson JA. 1997. Mechanism of gene expression by the glucocorticoid receptor: Role of protein–protein interactions. *Bioessays* **19:** 153–160.

Meijsing SH, Pufall MA, So AY, Bates DL, Chen L, Yamamoto KR. 2009. DNA binding site sequence directs glucocorticoid receptor structure and activity. *Science* **324:** 407–410.

Mortazavi A, Williams BA, McCue K, Schaeffer L, Wold B. 2008. Mapping and quantifying mammalian transcriptomes by RNA-Seq. *Nat Methods* **5:** 621–628.

Nissen RM, Yamamoto KR. 2000. The glucocorticoid receptor inhibits NFkappaB by interfering with serine-2 phosphorylation of the RNA polymerase II carboxy-terminal domain. *Genes & Dev* **14:** 2314–2329.

Niwa H, Burdon T, Chambers I, Smith A. 1998. Self-renewal of pluripotent embryonic stem cells is mediated via activation of STAT3. *Genes & Dev* **12:** 2048–2060.

Orth DN. 1995. Cushing's syndrome. *N Engl J Med* **332:** 791–803.

Pearce D, Yamamoto KR. 1993. Mineralocorticoid and glucocorticoid receptor activities distinguished by nonreceptor factors at a composite response element. *Science* **259:** 1161–1165.

Pratt WB, Morishima Y, Murphy M, Harrell M. 2006. Chaperoning of glucocorticoid receptors. *Handb Exp Pharmacol* **172:** 111–138.

Reimand J, Kull M, Peterson H, Hansen J, Vilo J. 2007. g:Profiler—a web-based toolset for functional profiling of gene lists from large-scale experiments. *Nucleic Acids Res* **35:** W193–W200.

Rhen T, Cidlowski JA. 2005. Antiinflammatory action of glucocorticoids—new mechanisms for old drugs. *N Engl J Med* **353:** 1711–1723.

Robertson G, Hirst M, Bainbridge M, Bilenky M, Zhao Y, Zeng T, Euskirchen G, Bernier B, Varhol R, Delaney A, et al. 2007. Genome-wide profiles of STAT1 DNA association using chromatin immunoprecipitation and massively parallel sequencing. *Nat Methods* **4:** 651–657.

Rogatsky I, Trowbridge JM, Garabedian MJ. 1997. Glucocorticoid receptor-mediated cell cycle arrest is achieved through distinct cell-specific transcriptional regulatory mechanisms. *Mol Cell Biol* **17:** 3181–3193.

Scheinman RI, Cogswell PC, Lofquist AK, Baldwin AS Jr. 1995. Role of transcriptional activation of Ikappa Balpha in mediation of immunosuppression by glucocorticoids. *Science* **270:** 283–286.

Smith AG, Heath JK, Donaldson DD, Wong GG, Moreau J, Stahl M, Rogers D. 1988. Inhibition of pluripotential embryonic stem cell differentiation by purified polypeptides. *Nature* **336:** 688–690.

So AY, Chaivorapol C, Bolton EC, Li H, Yamamoto KR. 2007. Determinants of cell- and gene-specific transcriptional regulation by the glucocorticoid receptor. *PLoS Genet* **3:** e94. doi: 10.1371/journal.pgen.0030094.

So AY, Cooper SB, Feldman BJ, Manuchehri M, Yamamoto KR. 2008. Conservation analysis predicts in vivo occupancy of glucocorticoid receptor-binding sequences at glucocorticoid-induced genes. *Proc Natl Acad Sci* **105:** 5745–5749.

Storey JD, Tibshirani R. 2003. Statistical significance for genomewide studies. *Proc Natl Acad Sci* **100:** 9440–9445.

Strähle U, Klock G, Schütz G. 1987. A DNA sequence of 15 base pairs is sufficient to mediate both glucocorticoid and progesterone induction of gene expression. *Proc Natl Acad Sci* **84:** 7871–7875.

Takahashi K, Yamanaka S. 2006. Induction of pluripotent stem cells from mouse embryonic and adult fibroblast cultures by defined factors. *Cell* **126:** 663–676.

Valouev A, Johnson DS, Sundquist A, Medina C, Anton E, Batzoglou S, Myers RM, and Sidow A. 2008. Genome-wide analysis of transcription factor binding sites based on ChIP-Seq data. *Nat Methods* **5:** 829–834.

Viegas LR, Hoijman E, Beato M, Pecci A. 2008. Mechanisms involved in tissue-specific apopotosis regulated by glucocorticoids. *J Steroid Biochem Mol Biol* **109:** 273–278.

Wang JC, Derynck MK, Nonaka DF, Khodabakhsh DB, Haqq C, Yamamoto KR. 2004. Chromatin immunoprecipitation (ChIP) scanning identifies primary glucocorticoid receptor target genes. *Proc Natl Acad Sci* **101:** 15603–15608.

Yamamoto T, Nakahata Y, Tanaka M, Yoshida M, Soma H, Shinohara K, Yasuda A, Mamine T, Takumi T. 2005. Acute physical stress elevates mouse period1 mRNA expression in mouse peripheral tissues via a glucocorticoid-responsive element. *J Biol Chem* **280:** 42036–42043.

Young JC, Hartl FU. 2002. Chaperones and transcriptional regulation by nuclear receptors. *Nat Struct Biol* **9:** 640–642.

Zhang Y, Liu T, Meyer CA, Eeckhoute J, Johnson DS, Bernstein BE, Nussbaum C, Myers RM, Brown M, Li W, et al. 2008. Model-based analysis of ChIP-Seq (MACS). *Genome Biol* **9:** R137. doi: 10.1186/gb-2008-9-9-r137.

Received June 9, 2009; accepted in revised form September 22, 2009.